An Improved and Novel De-Ramping Technique for Linear Frequency Modulated Continuous Wave Synthetic Aperture Radar

Farhad Arpanaei[1], Majid Shakeri[2], Behbod Ghalamkari[3]
[1]*Young Researcher and Elite Club, Central Tehran Branch, Islamic Azad University, Tehran, Iran.*
[2]*Young Researcher and Elite Club, Natanz branch, Islamic Azad University, Natanz, Iran.*
[3]*Computer and Electrical Engineering Department, Science and Research Branch, Islamic Azad University, Tehran, Iran.*
majid_shakeri@hotmail.com

***Abstract*—In this paper, a novel de-ramping technique for linear frequency modulated continuous wave (LFM-CW) synthetic aperture radar (SAR), named as the fixed delay de-ramping technique is introduced. The received and adaptive fixed delay version of transmitted signals was mixed to increase the processing gain of a system. Furthermore, in this study, the practical mode of de-ramping technique for LFM-CW SAR was considered against the related works assumed as the ideal mode. Similar to this work, the practical mode should consider the desired and undesired part of the de-ramped signal. In addition, the closed form equations for processing gain of the proposed de-ramping technique were derived. All in all, the simulation section illustrates a substantial improvement of the processing gain of the fixed de-ramping based on the proposed approach in comparison to the conventional methods.**

***Index Terms*—Fixed Delay De-Ramping Technique; Chirp Signal; Processing Gain; Linear Frequency Modulation; Continuous Wave; Synthetic Aperture Radar.**

I. INTRODUCTION

The SAR, with the features of all-weather, all-day imaging and fine penetrability, is widely used in military reconnaissance and civil fields [1]. The conventional SAR system usually uses pulse wave that can transmit a strong power, in which it transmits a signal within a short period of time and records the backscattering signal from targets [2]. However, the pulsed SAR systems are not suitable to be carried by light platforms because they must use high power generator to produce necessary high power pulses [3]. On the other hand, linear frequency modulated LFM-CW is able to achieve high performance with smaller structures and lower cost. Indeed, LFM-CW SAR will play significant role in future small low-cost high-resolution imaging radar applications [4]. In the LFM-CW SAR system, we use a LFM signal, named as the chirp signal, to mix a carrier wave as a reference. De-ramping on a receive technique is often used in LFM-CW SAR to obtain a very good range resolution. De-ramping technique consists of mixing the received signal with the transmitted signal to reduce the bandwidth of the echoes. The design of an offset intermediate frequency (IF) LFM-CW SAR de-ramping technique using a high-speed analog to digital convertor (ADC) and field-programmable gate array FPGA has been described in [5]. The offset de-ramping technique enables the use of better analog filters.

In [1], to generate the de-ramped signal, the transmitted signal was first partially mixed down using intermediate frequency (IF) frequency and filtered. This signal was then mixed with the received signal; the results of different components were similar to the ones in the traditional LFM-CW, although they were at an offset IF. With the signal of interest at a higher IF frequency, it is easier to find a high-Q filter that has linear phase, sharp cutoff frequencies, and better suppresses the feed-through. Hence, this study is based on this transceiver model. However, the practical mode of de-ramping technique was assumed to be the opposite of the ideal one in [6]. One challenging factor to the use of FM-CW SAR is the presence of nonlinearities in the transmitted signal. This causes to contrast- and range-resolution degradation, especially when the system is designed for high resolution long-range applications. Author in [7] presented a novel de-ramping processing technique, which eliminated the nonlinearity problem for the whole range profile. The derivation of processing gain, the desired and undesired part of de-ramped signal was not developed in [8]. The problem of the sources of the system error and the error tolerable levels for Ultra-Wide Band (UWB) SAR that adopt de-ramping technology was addressed in [3]. Moreover, the system error classification and error's effect on UWB SAR introduced according to the error's characteristics was presented in [9]. However, the author in [10] did not assume processing gain of his method. Along with this works, we assume that the received signal does not match perfectly on the transmitted version; hence, this dispatching phenomenon causes to degrade noticeably the processing gain of de-ramping technique. To deal with this problem, the desired and undesired part of de-ramped signal is considered, and we introduce a novel efficient de-ramping approach to address the delay in the de-ramping technique (FDDT). Additionally, to the best of the authors' knowledge, it is an initial attempt to derive the closed form formulation for de-ramping technique in LFM-CW SAR. The remainder of this paper is organised as follows. Section II presents the principle and basic contribution of an ideal and practical de-ramping technique, followed by the computational analysis in Section III. An ideal closed form formulation of processing gain derived for the proposed practical scheme is presented in Section IV. In Section V, we introduce the FDDT, and in Section VI and VII, an update of the previous equations according to FDDT's requirements is presented. Section VIII illustrates the simulation results for the proposed approach. Finally, the paper concludes with a brief summary of the results.

II. Principle of De-Ramping in FM-CW SAR

The choice of modulation scheme for radar's transmitted waveform is a design decision that must be made by the engineer. There are several different options, with their associated strengths and weaknesses, but a LFM chirp is chosen for this development because of its simplicity. The properties of the LFM chirp maybe utilised in order to simplify the range compression [1]. The conventional type waveform, which is usually used for FM-CW SAR is a saw tooth. The ramp is also known as a chirp (Figure 1). In Figure 1, BW is the signal bandwidth, an f_b defined as the beat frequency i.e., $f_b = \frac{BW}{PRI}\tau$ [3], where the PRI is the pulse repetition interval and $\tau$is is the delay between transmitted and received signals. The targets are illuminated by the antenna beam that reflects part of the transmitted signal back to the radar, where a receiving antenna collects this energy. The duration time of the signal travels to a target, at a distance and comes back to the radar is given by [3]:

$$\tau(t_{az}) = \frac{2R(t_{az})}{c} \tag{1}$$

where: c = Speed of light (~ 3×108 m/s)
R(.) = Time-variant distance of target from SAR
t_{az}= slow time or azimuth time

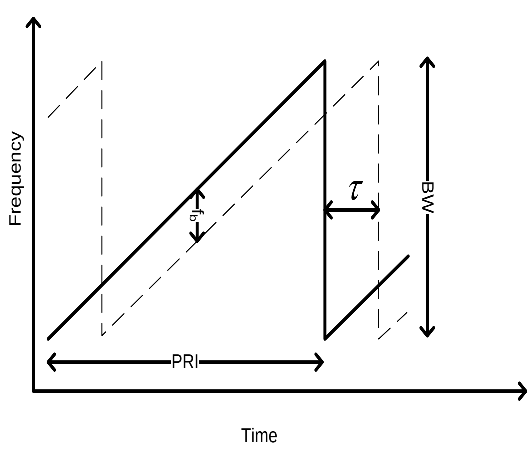

Figure 1: Chirp signal in the frequency–time domain. The (dashed) received signal is a delayed version of the (solid) transmitted one [3].

The form of the transmitted LFM chirp is given by [2]:

$$S_{trans}(t_r) = \exp\left\{ j2\pi\left(f_c - \frac{BW}{2}\right)t_r + \frac{k_r t_r^{\,2}}{2} + \varphi_0 \right\} \tag{2}$$

where: t_r = Fast time or range time
φ_0 = Initial phase
k_r = Chirp rate
f_c = Frequency center

In this paper, an ideal case is assumed, where the return signal from a target at range R (t_{az}) is simply a scaled and delayed copy of the transmitted signal. The return signal is written as [3]:

$$S_{rec}(t_r \cdot t_{az}) = A\exp\left\{ \begin{array}{l} j2\pi\left(\left(f_c - \frac{BW}{2}\right)(t_r - \tau(t_{az}))\right) \\ + \frac{k_r (t_r - \tau(t_{az}))^2}{2} + \varphi_0 \end{array} \right\} \tag{3}$$

where: A= Amplitude scaling of the received signal
BW= Bandwidth

Therefore, to avoid repetition of A as amplitude in the next equation, we consider A=1. However, the amplitude has affected the return signals due to reasons, such as speckle noise, etc. However, in our de-ramping analysis, when our focus is on the phase module, for simplicity, we assume that A=1 and the explicit dependence of $\tau(t_{az})$on $t_{az}$is dropped in the subsequent development. De-ramping is the process of mixing the received waveform with a copy of the transmitted waveform [2]. In the complex exponential notation, mixing and low-pass filtering is accomplished by multiplication with the complex conjugate, and it creates the de-ramped signal as $S_d(t_r . t_{az})$.

$$\begin{array}{l} S_d(t_r \cdot t_{az}) = S_{trans}(t_r) \times S^*_{rec}(t_r . t_{az}) = \\ \exp\left\{ j2\pi\left(\left(f_c - \frac{BW}{2}\right)t_r + \frac{k_r t_r^2}{2}\right)\right\} \\ \exp\left\{ -j2\pi\left(\left(f_c - \frac{BW}{2}\right)(t_r - \tau) - \frac{k_r (t_r - \tau)^2}{2}\right)\right\} = \\ \exp\left\{ j2\pi\left(\begin{array}{l} \left(f_c - \frac{BW}{2}\right)t_r + \frac{k_r t_r^2}{2} - \left(f_c - \frac{BW}{2}\right)t_r + \\ \left(f_c - \frac{BW}{2}\tau - \frac{k_r t_r^2}{2} + k_r t_r \tau - \frac{k_r \tau^2}{2}\right) \end{array} \right)\right\} = \\ \exp\left\{ j2\pi\left(\left(f_c - \frac{BW}{2}\right)\tau + k_r t_r \tau - \frac{k_r \tau^2}{2}\right)\right\} \end{array} \tag{4}$$

The mixing operation produces both the sum and difference of the two signals. Because the received signal from an ideal point target is a delayed copy of the transmitted LFM chirp, the sum of the two signals is a much higher frequency chirp, which is filtered out while the difference is simply a sinusoid with a frequency dependent on τ. If Equation (4) is split up, we can write:

$$S_d(t_r.t_{az}) = \exp\{j2\pi(k_r t_r \tau)\} \exp\left\{ j2\pi\left(\left(f_c - \frac{BW}{2}\right)\tau - \frac{k_r\tau^2}{2}\right)\right\} \quad (5)$$

The first exponential term is the range-dependent sinusoid, referred to the beat signal, while the second exponential contains range-dependent phase terms, which accounts for the LFM chirp in the azimuth direction. The beat or intermediate frequency is defined as:

$$f_b \underline{\Delta} k_r \tau = \frac{2k_r R(\tau)}{c} \quad (6)$$

Once the data has been de-ramped, the range compression is accomplished by taking the Fourier transform of Equation (5). In actual SAR processing, the data is sampled so that a discrete Fourier transform must be used in frequency range direction. Since this development is for illustration purposes only, a continuous Fourier transform is used.

$$S_D(f_r) = F\left[\begin{array}{l}\exp\{j2\pi(k_r t_r \tau)\}\cdot \\ \exp\left\{ j2\pi\left(\left(f_c - \frac{BW}{2}\right)\tau - \frac{k_r\tau^2}{2}\right)\right\}\end{array}\right] =$$
$$\exp\left\{ j2\pi\left(\left(f_c - \frac{BW}{2}\right)\tau - \frac{k_r\tau^2}{2}\right)\right\}.\int_{-\infty}^{+\infty}\exp\{j2\pi(k_r t_r \tau)\}dt_r \quad (7)$$
$$= \exp\left\{ j2\pi\left(\left(f_c - \frac{BW}{2}\right)\tau - \frac{k_r\tau^2}{2}\right)\right\}\delta(f_r - k_r\tau)$$

where f_r= Frequency in the range direction
$S_D(f_r)$ = The Fourier transform of $S_d(t_r)$

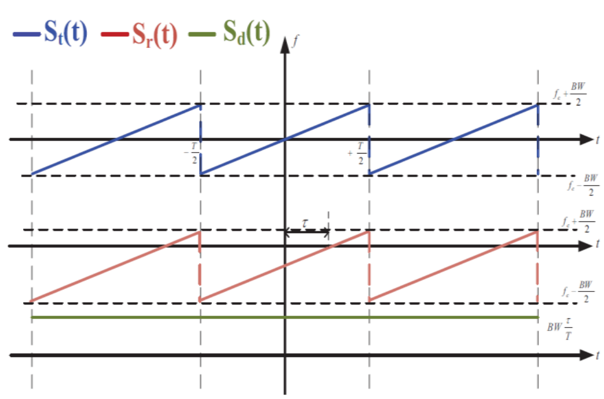

Figure 2: Frequency-time representation of transmitted, received and de-ramped signals for ideal de-ramping technique.

The delta function is maximized when $f_r = k_r\tau$. The practical result is that the range compressed data, which is the frequency domain representation of the de-ramped data, contains local maxima at frequencies which correspond directly to range-to-target values. Notice that this process decreases the computational load required for the range compression since it can be accomplished by taking a fast Fourier transform (FFT) of the data along the range dimension [11]. Figure 2 illustrates the de-ramping of an LFM signal.

III. Processing Gain Due to the De-Ramping Technique

In Section II, the discussion on an ideal de-ramping technique has been introduced. One can see that the bandwidth of received signal was decreased in the range direction e.g., ideal de-ramping technique. In the literature [3-7], the authors assumed that both of the transmitted and received signal are perfectly matched to each other. In Figure 3, the presentation of an ideal de-ramping technique and the concept of perfect matching are illustrated. In many ideal cases, this model in LFM-CW SAR processing algorithms is applied. However, in practical cases, if one can apply this model, he deals with some problems. In fact, because of the transmitted signal is periodic, the de-ramping technique causes some distortions, which is assumed as the undesired part in this study. Figure 3 shows the LFM transmitted signal$S_{trans}(t_r)$, received signal $S_{rec}(t_r.t_{az})$ and the de-ramped signal$S_d(t_r.t_{az})$ in frequency, respectively.

As shown in Figure 3, the periodic phenomenon for the received and de-ramped signals is not considered and the de-ramped signal is constant. Hence, as will be seen in the following, the processing gain of ideal de-ramping technique will be high and impractical. In Section II, the related equations for an ideal de-ramping technique are listed from Equation (2) to Equation (7). In order to improve the ideal de-ramping technique and in practical cases, we must consider Figure 4. Figure 4 also shows the $S_{trans}(t_r)$, $S_{rec}(t_r.t_{az})$ and$S_D(t_r.t_{az})$, in practical mode, respectively.

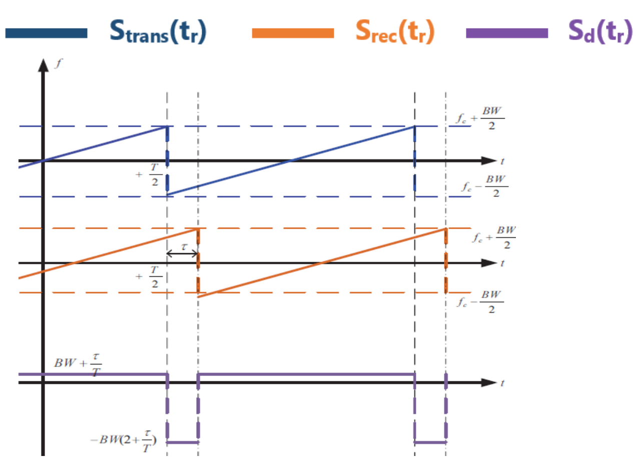

Figure 3: The frequency-time representation of transmitted, received and de-ramped signals for practical de-ramping technique.

In order to compute the processing gain (PG) of the practical de-ramping technique, the transmitted and received signal in Equation (8) and Equation (9) is rewritten, respectively. It is noted that, in Figure 3 the delay of echo signal is considered as τ. Therefore, based on the time duration as shown in Figure 3, one can write:

$$S_{trans}(t_r) = \exp\left\{ j2\pi\left(\left(f_c - \frac{BW}{2}\right)t_r + \frac{k_r t_r^2}{2}\right)\right\} \quad \frac{nT}{2} \le t < \frac{(n+2)T}{2} \tag{8}$$

$$S_{rec}(t_r.t_{az}) = \begin{cases} \exp\left\{ j2\pi\left(\begin{array}{l}\left(f_c - \frac{BW}{2}\right)(t_r - T - \tau) \\ + \frac{k_r(t_r + T - \tau)^2}{2}\end{array}\right)\right\} \\ ; \quad \frac{nT}{2} \le t < \frac{nT}{2} + \tau \\ \exp\left\{ j2\pi\left(\begin{array}{l}\left(f_c - \frac{BW}{2}\right)(t_r - \tau) \\ + \frac{k_r(t_r - \tau)^2}{2}\end{array}\right)\right\} \\ ; \quad \frac{nT}{2} + \tau \le t < \frac{(n+2)T}{2} \end{cases} \tag{9}$$

where: T = time duration of transmitted pulse
BW=Bandwidth
n = Number of pulses.

Based on Equation (4), one can write the de-ramped signal as:

$$S_d(t_r.t_{az}) = \begin{cases} \exp\left\{ j2\pi\left(f_c - \frac{BW}{2}\right)(T - \tau) - \frac{k_r(T-\tau)^2}{2} - k_r t_r (T - \tau)\right\} \\ ;\frac{nT}{2} \le t < \frac{nT}{2} + \tau \\ ; \quad \exp\left\{ j2\pi\left(\left(f_c - \frac{BW}{2}\right)\tau - \frac{k_r \tau^2}{2} + k_r t_r \tau\right)\right\} \\ ; \quad \frac{nT}{2} + \tau \le t < \frac{(n+2)T}{2} \end{cases} \tag{10}$$

According to Equation (10) and Figure 4, the de-ramped signal consists of two parts: the first part is named as the desired part and the second one is named as the undesired part. Although in ideal or conventional de-ramping model as shown in Figure 3, the undesired part is not considered. Here after the desired part of the de-ramped signal is showed as $S_D^{desired}(t_r.t_{az})$ and the undesired part as $S_D^{undesired}(t_r.t_{az})$.

A. The Processing Gain of Desired De-ramped Signal(PGDD)

In order to calculate PGDD, we should rewrite the Equation (10) as below:

$$S_d^{desired}(t_r.t_{az}) = \begin{cases} 0; \quad \frac{nT}{2} \le t < \frac{nT}{2} + \tau \\ \exp\left\{ j2\pi\left(\left(f_c - \frac{BW}{2}\right)\tau - \frac{k_r \tau^2}{2} + k_r t_r \tau\right)\right\} \\ ; \quad \frac{nT}{2} + \tau \le t < \frac{(n+2)T}{2} \end{cases} \tag{11}$$

By converting Equation (11) to discrete time domain and then applying Fourier transform to it, we are able to power the zspectral density (PSD) of the desired de-ramped signal in Equation (12).

$$S_d^{desired}(f_r) = \frac{1}{N}\sum_{n=1}^{N} S_d^{desired}[n].\exp(-j2\pi f_n);\ f \in \left\{ \frac{\left\lfloor \frac{-N}{2} \cdots \frac{N}{2} - 1 \right\rfloor}{N} \right\} \tag{12}$$

where: $N = f_s \times T$
f_s= Sampling frequency
T = Transmitted signal duration

By substituting the Equation (11) to Equation (12), desired part can write as (13):

$$S_d^{desired}(f_r) = \frac{1}{N}\sum_{n=1}^{N} \exp\left\{ j2\pi\left(\begin{array}{l}\left(f_c - \frac{BW}{2}\right)\tau \\ - \frac{k_r \tau^2}{2} + k_r n \tau\end{array}\right)\right\} \exp(-j2\pi f_n) \tag{13}$$

In Equation (13), $S_d^{desired}(f_r)$ is zero for all n ∈ [1…Nτ] where: $N_\tau = f_s \tau$
n= Discrete time

Based on Equation (14) as follow:

$$\frac{1}{N}\sum_{n=1}^{N} \exp(-jnx) = \exp\left(-j\frac{(N+1)x}{2}\right)\frac{\sin\frac{Nx}{2}}{\sin\frac{x}{2}} \tag{14}$$

one can conclude that the Equation (13) is equal to:

$$S_d^{desired}(f_r) = \exp\left\{ j2\pi\left(\left(f_c - \frac{BW}{2}\right)\tau - \frac{k_r \tau^2}{2}\right)\right\} .\exp\left\{ -j2\pi(f_r - k_r\tau)\left(\frac{N - N_r + 1}{2}\right)\right\} .\frac{\sin(\pi(N - N_r + 1)(f_r - k_r\tau))}{N.\sin(\pi(f_r - k_r\tau))} \tag{15}$$

Now in order to express PGDD, we should assume the maximum absolute of Equation (15), which is given by:

$$\left|S_d^{desired}(f_r)\right| = \frac{\sin(\pi(N-N_r+1)(f_r-k_r\tau))}{N.\sin(\pi(f_r-k_r\tau))} \quad (16)$$

By applying some basic mathematical theories and lemma's, the PGDD can be defined as:

$$PGDD \triangleq \left|S_d^{desired}(f_r)\right|_{f_r=k_r\tau} = \frac{N-N_r+1}{N} \quad (17)$$

B. Processing Gain of Undesired De-Ramped Signal (PGUD)

In order to compute PGUD, we rewrite the undesired part of signal in Equation (10), given that:

$$PGDD \triangleq \left|S_d^{desired}(f_r)\right|_{f_r=k_r\tau} = \frac{N-N_r+1}{N}$$

$$S_d^{undesired}(t_r.t_{az}) = \begin{cases} \exp\left\{ j2\pi \left(\left(f_c - \frac{BW}{2}\right)(T-\tau) - \frac{k_r(T-\tau)^2}{2} - k_r t_r (T-\tau) \right) \right\}; \\ \frac{nT}{2} \le t < \frac{nT}{2} + \tau \\ 0; \quad \frac{nT}{2} + \tau \le t < \frac{(n+2)T}{2} \end{cases} \quad (18)$$

Considering that $S_d^{desired}(f_r)$ is zero for all $n \in [1 \ldots N_\tau]$ with the same operations in subsection (III.A), one can conclude that:

$$\left|S_d^{undesired}(f_r)\right| = \frac{\sin(\pi(N_r+1)(f_r+k_r(T-\tau)))}{N.\sin(\pi(f_r+k_r(T-\tau)))} \quad (19)$$

Again, by applying some basic mathematical theories and lemma's, one can conclude that:

$$PGUD \triangleq \left|S_d^{undesired}(f_r)\right|_{f_r=k_r(T-\tau)} = \frac{N_r+1}{N} \quad (20)$$

IV. Total Processing Gain (TPG)

According to the aforementioned discussion, the total processing gain of LFM-CW SAR can be defined as below:

$$TPG \triangleq \frac{\left|S_D^{undesired}(f_r)\right|_{f_r=k_rT}}{\left|S_D^{undesired}(f_r)\right|_{f_r=k_r(T-\tau)}} = \frac{\frac{N-N_r+1}{N}}{\frac{N_r+1}{N}} = \frac{N-N_r+1}{N_r+1} \quad (21)$$

As seen in Figure 3 and its related equations in Section II for ideal case of de-ramping technique, the TPG for ideal mode is N+1, which is higher and it is not feasible. However, by considering the practical case, one can achieve a reasonable TPG. As shown in the practical de-ramping technique, the PG is not uniformly distributed. In order to overcome this problem, a new strategy for de-ramping technique named fixed delay de-ramping technique or FDDT is proposed. In FDDT mode, there is a delay of the transmitted signal by considering the center cell position in the range direction. As shown in the following, the TPG of FDDT or TPG_{FDDT} is more efficient than TPG of practical de-ramping technique.

V. Total Processing Gain of Fixed Delay De-Ramping Technique (TPG-FDDT)

Based on the aforementioned discussion in SAR applications, when the received signal is scattered from far and near range (the beginning and the end of swath), the PG of echo signal does not uniformly distribute along the swath. In this manner, the echo signals of swath's beginning have higher PG than the ones reflected from the end of swath. To overcome this problem, a delay of transmitted signal before to mix by echo signal (de-ramping process) is vital. In order to clarify this issue, one can exploit a numerical and practical example by assuming that the R_{min} which is related to the beginning of swath range is equal to 1000 m and the R_{max} which is related to the end of swath range is 2000 m. In this situation, by setting T=1 msec, fc=9.6 GHz, BW=200 MHz and fs=2.5×fc , the sample delay due to these range is calculated as:

$$\tau_{min} = \frac{2 \times R_{min}}{c} = \frac{2 \times 1000}{3 \times 10^8} = 6.6\mu\sec \quad (22)$$

$$\tau_{max} = \frac{2 \times R_{max}}{c} = \frac{2 \times 2000}{3 \times 10^8} = 13.3\mu\sec \quad (23)$$

Therefore, the N is equal to 24×106, $N_{\tau_{min}} = 6.6 \times 10^{-6} \times 24 \times 10^9 = 16 \times 10^4$ and $N_{\tau_{max}} = 32 \times 10^4$. Now based on Equation (21), one can write:

$$TPG_{max} \approx \frac{N}{\tau_{min}} \approx \frac{24 \times 10^6}{16 \times 10^4} \approx 43.5dB \quad (24)$$

$$TPG_{min} \approx \frac{N}{\tau_{max}} \approx \frac{24 \times 10^6}{32 \times 10^4} \approx 37.5dB \quad (25)$$

As you can see in Equation (24) and Equation (25), the PG difference between the beginning and the end of the swath range, it is approximately 6 dB. In other words, any cell position in the range direction introduces exclusive TPG, which is different from another one. By applying the FDDT, the TPG and distributing the TPG among the range, bins can be uniformly and symmetrically improved. The amount of this dilation is selected according to the center of swath range. In Figure 4 the block diagram of the FDDT is illustrated based on [4]. As shown in Figure 4, before mixing the transmitted signal by the received signal, a fixed delay applies to the transmitted signal. Furthermore, in this study both the desired and undesired de-ramped signals are considered.

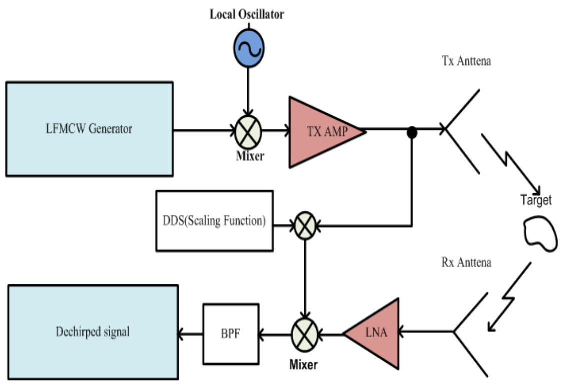

Figure 4: The block diagram of novel proposed de-ramping approach

VI. Update the Equations in Fixed Delay De-Ramping Technique

Based on Figure 4, the reference signal is the fixed delay version of transmitted signal, which is mixed by echo signal in the FDDT approach. Hence, it is written as:

$$S_{ref}(t_r.\tau_c) = \exp\left\{ j2\pi\left(\left(f_c - \frac{BW}{2}\right)(t_r - \tau_C) + \frac{k_r(t_r - \tau_c)^2}{2}\right)\right\} \quad (26)$$

With respect to the conventional de-ramping concept, which has been discussed above, the fixed delay de-ramped signal is given by:

$$S_d(t_r.t_{az}) = \begin{cases} \exp\left\{ j2\pi\left(\begin{array}{l}\left(f_c - \frac{BW}{2}\right)(T-(t_r-\tau_C)) - \\ \frac{k_r(T-(t_r-\tau_c))^2}{2} - \\ k_r t_r (T-(\tau-\tau_c))\end{array}\right)\right\}; \\ \frac{nT}{2} \le t < \frac{nT}{2} + \tau \\ \exp\left\{ j2\pi\left(\begin{array}{l}\left(f_c - \frac{BW}{2}\right)(t_r-\tau_C) - \\ \frac{k_r(t_r-\tau_c)^2}{2} + \\ k_r t_r (\tau-\tau_c)\end{array}\right)\right\}; \\ \frac{nT}{2} + \tau \le t < \frac{(n+2)T}{2} \end{cases} \quad (27)$$

According to Equation (16) and Equation (19), the $\left|S_D^{desired}(f_r)\right|$ and $\left|S_D^{undesired}(f_r)\right|$ are updated to Equation (28) and Equation (29), respectively.

$$\left|S_{FD}^{desired}(f_r)\right| = \frac{\sin(\pi(N-(N_r-N_{\tau c})+1)(f_r - k_r(\tau-\tau_c)))}{N.\sin(\pi(f_r - k_r(\tau-\tau_c)))} \quad (28)$$

$$\left|S_{FD}^{undesired}(f_r)\right| = \frac{\sin(\pi(N_\tau - N_{\tau c}+1)(f_r - k_r(T-(\tau-\tau_c))))}{N.\sin(\pi(f_r + k_r(T-(\tau-\tau_c))))} \quad (29)$$

where: $N_{\tau c} = f_s \times \tau_c$

$$\tau_c = \frac{2R_{center}}{C}$$

By applying the same method used in the Section 3, the TPG_{FDDT} can be calculated as below:

$$TPG_{FDDT} = \frac{\left|S_{FD}^{desired}(f_r)\right|_{f_r = k_r(\tau-\tau_C)}}{\left|S_D^{undesired}(f_r)\right|_{f_r = -k_r(T-(\tau-\tau_C))}} = \frac{\frac{N-(N_\tau - N_{\tau C})+1}{N}}{\frac{(N_\tau - N_{\tau C})+1}{N}} = \frac{N-(N_\tau + 1 - N_{\tau C})}{N_r + 1 - N_{\tau C}} \quad (30)$$

Now, returning to the aforementioned numerical example, where it has just assumed R_{center} =1500 m, therefore N_{τ_c} is equal to $\frac{2\times1500}{3\times10^8} \times 24 \times 10^9 = 24 \times 10^4$. Based on Equation (30), the Equation (24) and Equation (25) are exchanged to:

$$TPG_{FDT} \approx \left|\frac{N}{N_{\tau\min} - N_{\tau c}}\right| \approx \left|\frac{N}{N_{\tau\max} - N_{\tau c}}\right| \approx \frac{24\times10^6}{(24-16)\times10^4} \approx \frac{24\times10^6}{(32-24)\times10^4} \approx 49.5dB \quad (31)$$

By comparing the amount of TPG_{FDDT} in Equation (31) with the TPG in Equation (24) and Equation (25), one can conclude that the fixed delay results in an improvement in the PG of de-ramping process about 6 dB. Further, the FDDT approach results in every range bin to have the same efficient PG and symmetrically distributed along the range direction.

VII. Simulation Results

This section presents the simulation results of a comparison between the PG of the conventional de-ramping technique in the ideal approach (CDTI) when the undesired part is not considered and the conventional de-ramping technique in practical approach (CDTP) when both the desired and undesired parts are considered and the FDDT is applied.

In this paper, f_c, BW and pulse repetition frequency (PRF) are set to 9.6 GHz, 200 MHz and 1000 Hz, respectively. Considering the CW-SAR system and the PRF, the time duration of transmitted signal is 1 msec. Additionally, three point targets are assumed, namely, A, B and C, which are located at 100 meter in blue, 5000 meter in pink and 10000 meter in green from the platform, respectively. Figure 5 shows the PG of CDTI, which shows the undesired effect of the de-ramping technique, achieving to more and impractical PG.

Based on Equation (21), when $N_\tau=0$, then $PG = \log N = 126$ dB. Moreover, the simulated results in Figure 6 validate this matter. It should be noted that we consider the targets are far from each other, showing an obvious distinction of the targets across the spectrum. Figure 6 is a zoomed version of Figure 5 to distinguish the targets conveniently. With regard to CDTP, Figure 7 illustrates the spectrum of these targets in terms of range bins. According to Figure 7, the PG of the left targets is different from each other when the CDTP approach is applied, but for the right targets when the CDTI considers the same PG.

Based on the aforementioned numerical example in the last section, the differences between the targeted PGs, which is about 40 dB (refer to Figure 8 where $63^{(dB)}$-$22^{(dB)}$= 41dB) due to the application of the FDDT can be reduced. As shown in Figure 8, the amount of PG for target A and C in FDDT approach is 29 dB because they have the same position to the reference point, which is located in the range 1500 m (R_{center} =1500 m) i.e., it should be mentioned that these targets have the same distance from the center of swath. Further, the amount of TPG_{FDDT} for target B is 103 dB. Owing to the perfect matching of reference and received signal for target B, it has most TPG_{FDDT} among the others. However, in FDDT approach, the PG is not uniformly distributed along the range bins in comparison to the CDTP without FDDT. It is clear that the TPG_{FDDT} is improved about 6 dB in the worst case (compared to Equation (31) and Equation (24)).

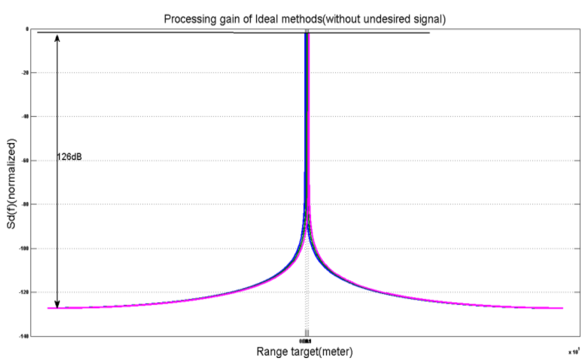

Figure 5: PG of de-ramped signal without undesired signal (CDTI).

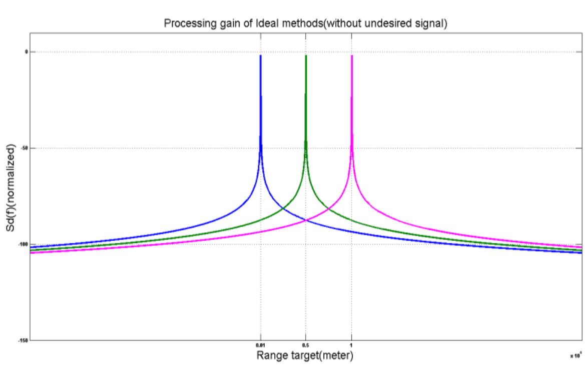

Figure 6: Processing Gain of de-ramped signal without undesired signal (CDTI) - Zoomed Version.

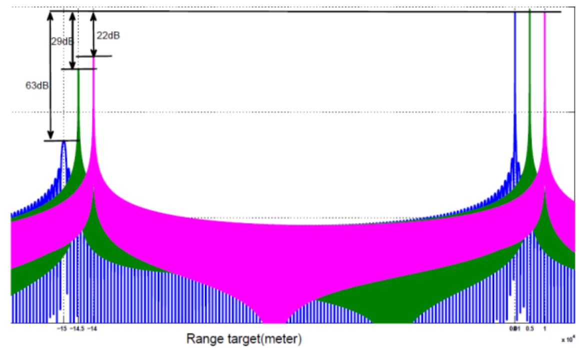

Figure 7: The Output De-ramped signal for left targets by applying CDTP (without FDDT) and right targets by applying CDTI.

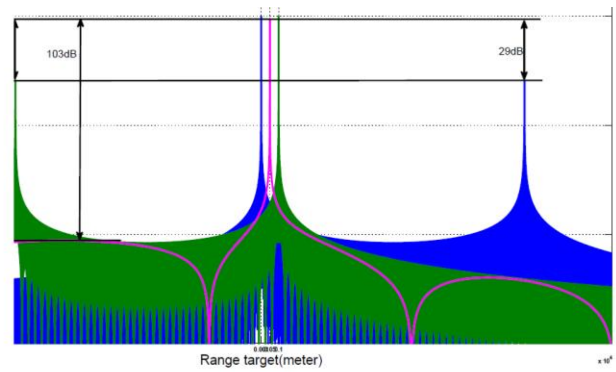

Figure 8: The Output De-ramped signal for targets in 100 (blue), 5000(pink) and 10000(green) meter in CDTP (with FDDT).

VIII. Conclusion

De-ramp (de-chirp) on receive is often used in LFM-CW SAR. In order to decline the sampling frequency, and then to decrease the data in the range direction, the radar demodulates the received signal by mixing it by an echo of the delayed transmitted waveform. In this paper, the closed form formulations for processing the gain of a novel de-ramping scheme for LFM-CW SAR is derived. Accordingly, the new approach has been introduced, namely, the FDDT.

The results of our simulations demonstrated that FDDT could dramatically increase the PG of the de-ramping technique compared to the conventional approach. However, the former proposed approach causes the PG to be symmetrically and uniformly distributed along the range bins. In addition, in relation to the previous works, both desired and undesired part of transmitted and received continuous chirp signals were considered. The simulation outcomes showed that the proposed FDDT scheme increases the PG of de-ramping technique approximately 41 dB compared to the practical and conventional de-ramping method. Moreover, by appropriately exploiting the properties of the chirp scaling, the adaptive delay of transmitted signal was efficiently performed.

References

[1] W.-g. Chang and Z.-m. Zhou, "The analysis of UWB SAR system error," in Aerospace and Electronics Conference, 1997. NAECON 1997., Proceedings of the IEEE 1997 National, 1997, pp. 964-969.

[2] C. Clemente and J. J. Soraghan, "Fractional Range Doppler Algorithm for SAR imaging," in Radar Conference (EuRAD), 2010 European, 2010, pp. 248-251.

[3] Z. Jiang, F. Huang, J. Wan, and Z. Cheng, "Modified frequency scaling algorithm for FMCW SAR data processing," Chinese Journal of Aeronautics, vol. 20, pp. 339-345, 2007.

[4] Z.-H. Jiang, K. Huang-Fu, and J.-W. Wan, "A chirp transform algorithm for processing squint mode FMCW SAR data," IEEE Geoscience and Remote Sensing Letters, vol. 4, pp. 377-381, 2007.

[5] A. Meta and P. Hoogeboom, "Development of signal processing algorithms for high resolution airborne millimeter wave FMCW SAR," in IEEE International Radar Conference, 2005., 2005, pp. 326-331.

[6] A. Meta, P. Hoogeboom, and L. P. Ligthart, "Signal processing for FMCW SAR," IEEE Transactions on Geoscience and Remote Sensing, vol. 45, pp. 3519-3532, 2007.

[7] G. Shu-min, C. Zhu, and H. Kan, "Study on imaging algorithm of De-chirped FM-CW SAR," in 2006 CIE International Conference on Radar, 2006, pp. 1-4.

[8] C. Stringham, D. G. Long, B. Wicks, and G. Ramsey, "Digital receiver design for an offset IF LFM-CW SAR," in 2011 IEEE RadarCon (RADAR), 2011, pp. 960-964.

[9] Y. Wang, C. Qu, D. Ping, and B. Chen, "An Improved RD Imaging Algorithm for FMCW SAR," in 2008 4th International Conference on Wireless Communications, Networking and Mobile Computing, 2008, pp. 1-4.

[10] D. Zhu, M. Shen, and Z. Zhu, "Some aspects of improving the frequency scaling algorithm for dechirped SAR data processing," IEEE Transactions on Geoscience and Remote Sensing, vol. 46, pp. 1579-1588, 2008.